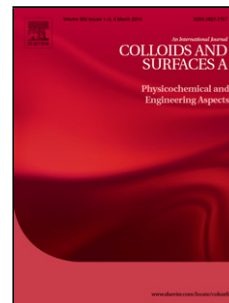


Accepted Manuscript

Title: Influencing the texture and morphological properties of layered double hydroxides with the most diluted solvent mixtures – the effect of 6-8 carbon alcohols and temperature

Authors: Szabolcs Muráth, Márton Szabados, Dániel Sebők, Ákos Kukovecz, Zoltán Kónya, István Szilágyi, Pál Sipos, István Pálinkó



PII: S0927-7757(19)30176-1
DOI: <https://doi.org/10.1016/j.colsurfa.2019.04.053>
Reference: COLSUA 23397

To appear in: *Colloids and Surfaces A: Physicochem. Eng. Aspects*

Received date: 27 February 2019
Revised date: 15 April 2019
Accepted date: 19 April 2019

Please cite this article as: Muráth S, Szabados M, Sebők D, Kukovecz Á, Kónya Z, Szilágyi I, Sipos P, Pálinkó I, Influencing the texture and morphological properties of layered double hydroxides with the most diluted solvent mixtures – the effect of 6-8 carbon alcohols and temperature, *Colloids and Surfaces A: Physicochemical and Engineering Aspects* (2019), <https://doi.org/10.1016/j.colsurfa.2019.04.053>

This is a PDF file of an unedited manuscript that has been accepted for publication. As a service to our customers we are providing this early version of the manuscript. The manuscript will undergo copyediting, typesetting, and review of the resulting proof before it is published in its final form. Please note that during the production process errors may be discovered which could affect the content, and all legal disclaimers that apply to the journal pertain.

Influencing the texture and morphological properties of layered double hydroxides with the most diluted solvent mixtures – the effect of 6-8 carbon alcohols and temperature

Szabolcs Muráth^{a,b*}, Márton Szabados^{c,d}, Dániel Sebők^e, Ákos Kukovecz^f,
Zoltán Kónya^{f,g}, István Szilágyi^{a,b}, Pál Sipos^{b,h}, István Pálinkó^{c,d}

^a MTA-SZTE Lendület Biocolloids Research Group, University of Szeged, 1 Rerrich Béla tér, H-6720 Szeged, Hungary

^b Interdisciplinary Excellence Centre, Department of Physical Chemistry and Materials Science, University of Szeged, 1 Rerrich Béla tér, H-6720 Szeged, Hungary

^c Material and Solution Structure Research Group, Institute of Chemistry, University of Szeged, 1 Aradi vértanúk tere, H-6720 Szeged, Hungary

^d Department of Organic Chemistry, University of Szeged, 8 Dóm tér, H-6720 Szeged, Hungary

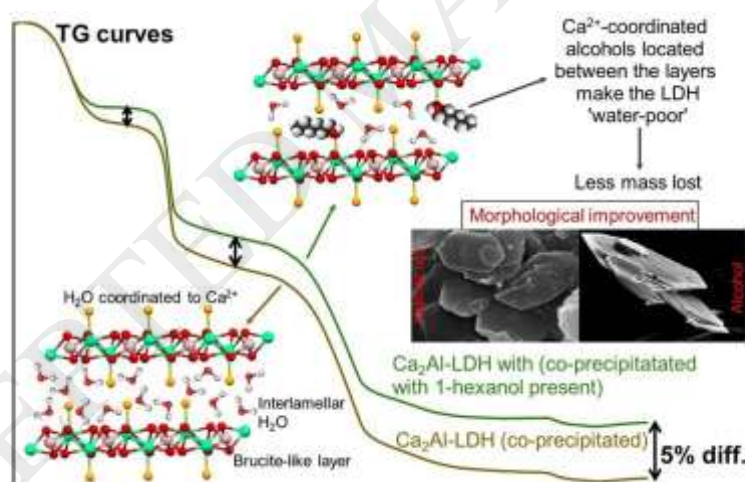
^e Interdisciplinary Excellence Centre, Department of Applied and Environmental Chemistry, University of Szeged, 1 Rerrich Béla tér, H-6720 Szeged, Hungary

^f Department of Applied and Environmental Chemistry, University of Szeged, 1 Rerrich Béla tér, H-6720 Szeged, Hungary

^g MTA-SZTE Lendület Reaction Kinetics and Surface Chemistry Research Group, 1 Rerrich Béla tér, H-6720 Szeged, Hungary

^h Department of Inorganic and Analytical Chemistry, University of Szeged, 7 Dóm tér, H-6720 Szeged, Hungary

Graphical abstract



Abstract Three layered double hydroxides (MgAl-, CaAl- and CaGa-LDH) were obtained *via* co-precipitation with NaOH as base, and the effects of ageing in the slurry at elevated temperatures were under investigation. As expected, the crystallinity of the products improved after ageing, and the particle diameter of the Ca-containing samples grew as well. The experiments were carried out in the presence of either 1-hexanol, 1-heptanol or 1-octanol during the LDH formation. Each alcohol, functioning as a co-solvent in low concentration, had the same impact on the crystalline properties of the product: the morphology of all LDHs improved and the diameter of the CaM-LDH particles (M = Al, Ga) increased from the original 100-300 nm to 1-3 μ m without ageing to an immense 5-10 μ m after treatment at 60 °C. Small changes were detected in the X-ray traces, the basal spacing of the CaM-LDHs shrank. Considering the

presence of large alcohol molecules in the interlamellar space, one may predict a rise in the basal spacing, however, it is also a function of the hydration degree of the interlayer space. Since alcohols with 6-8 carbon atoms are regarded as hydrophilic ones, we attribute the smaller interlayer distance to the partial exclusion of water from the interlamellar space. This phenomenon was confirmed *via* thermogravimetry. The difference in the size of alcohol and heat-treated CaM-LDHs to MgAl-LDH presumably arise from the stronger interaction of calcium ions with structural alcohol molecules due higher coordination number of the calcium ion (7) in the corresponding LDHs than that for the magnesium or aluminium ions (6).

Keywords Layered double hydroxides (LDHs), Effect of alcohols, X-ray and microscopic characterization, Symmetrical morphology, Co-precipitation synthesis, Thermal analysis

* Corresponding author's e-mail address: muratsz@chem.u-szeged.hu (Szabolcs Muráth)

1. Introduction

Inorganic, anionic clay-type layered double hydroxides (LDHs) are naturally occurring lamellar materials. The structure of their general representatives may be derived from the structure of the also lamellar brucite, *i.e.* Mg(OH)₂: a portion of divalent cations is replaced by trivalent ones, giving the layers excess positive charge, which is neutralized by the interlamellar (intercalated) anions. The general formula obtained is as follows: [M²⁺_{1-x}M³⁺_x(OH)₂][Aⁿ⁻_xmH₂O], where M²⁺ and M³⁺ are divalent and trivalent metal ions and Aⁿ⁻_xmH₂O is the charge-compensating anion, mostly in hydrated form [1]. The most common structure-building metals for M²⁺ and M³⁺ are Mg, Fe, Cu, Zn, Ca, Ni and Al, Cr, Fe, Co, respectively [2]. The widespread applicability of LDHs emerge from multiple factors: facile anion exchange with a large variety of anions [3,4], various metallic composition [2], biocompatibility [5], stability of inorganic and organic-inorganic hybrid materials [6-8] and the basicity of their derived oxides and the LDHs themselves [9]. Hence, they can be applied as adsorbents for water and air purification [10, 11], catalysts [12], drug and catalyst carriers [13,14], capacitors [15], light emitters [16], etc. The morphology of LDH grains is often irregular or has a distorted hexagonal symmetry with a typical diameter in the submicron range. However, synthetic techniques involving high temperature are suitable for preparing highly symmetrical crystals, occasionally with remarkable size. Such processes involve urea hydrolysis method and hydrothermal treatment or their combination. Co-precipitation is executed by the intrinsic basic property of NaOH, while urea decomposes in two steps to NH₃ and formaldehyde from 60 °C. Carrying out the hydroxide formation at room temperature (*via* the conventional co-precipitation with NaOH) and applying post-synthetic hydrothermal treatment result in a product within the usual size distribution (Case 1), high-temperature syntheses (urea method or precipitation in hydrothermal conditions) yield crystals with high geometric parameters (Case 2); nevertheless, particle size distribution is always narrowed by ageing. Case 1 is favoured when the size is better kept small. This is either required when potential human applications are in sight [17] (large particles can damage tissue cells and capillaries) or when higher specific surface area is important, (*e.g.* for water treatment [18]). The effect of Case 2-type processes has been published several occasions, and it was found that

bigger platelets are obtained with higher temperatures and longer ageing [19,20]. A comparative study was also conducted to reveal the differences between Case 1 and Case 2 [21]. It was communicated that the average particle size is tenfold with urea hydrolysis when it was used with similar ageing time and temperature, even with higher initial metal ion concentration. For lower concentrations, the growth is even more prominent. These papers examine Mg_2Al -LDHs, but recently Ca_2Al -LDH was prepared at elevated temperatures and pressures in a continuous manner, and the effect observed was the same as for Mg_2Al -LDH [22]. Earlier, hydrothermal method was utilized to produce single crystals from two different Ca_2Al -LDHs, although starting from solid, not dissolved precursors [23,24].

Another method uses aqueous miscible organic co-solvents to aid the formation of highly crystalline LDHs. When five different alcohols were under consideration, it was concluded that primary alcohols (methanol and ethanol) and ethylene glycol had minimal effect on the crystallinity of Mg_2Al -LDH, but glycerol and pentaerythritol led to products with lower qualities [25]. We must note that not only water, but other solvent molecules can be present between the layers. Polyols make stronger interactions with water molecules than mono- or dihydroxy alcohols making the interlamellar space richer in water, but altogether, the result is a weaker and less-ordered stacking of the brucite-like layers. Despite the hydrothermal treatment, the LDHs from aqueous methanolic and ethanolic solutions share the same grain size as the as-prepared one from pure water. The favourable effect of ethanol (on $CoNi_4$ -LDH [26]) and ethylene diamine (on Mg_2Al -LDH [27]) was also demonstrated before. Beside their useful co-solvent role, organic solvents are also known to disrupt the structure of the LDHs inducing partial or total exfoliation of the platelets. Mainly formamide [28] and 1-butanol [29] is applied for such procedures, albeit the efficiency of other amides was also shown [30].

In our contribution, we report the improvement in crystal quality for Mg_2Al -LDH, Ca_2Al -LDH and Ca_2Ga -LDH synthesized by co-precipitation with 1-hexanol, 1-heptanol or 1-octanol also present in the reaction mixture in saturation concentration. The thermal behaviour of the materials is also revealed, and the phase analysis of the mixed oxides was performed. To the best of our knowledge, this is the first published research to examine the nitrate form of Ca_2Ga -LDH, after an X-ray study conducted on its chloride form in 2002 [31].

2. Materials and methods

2.1 Starting materials

High-purity $\text{Ca}(\text{NO}_3)_2 \cdot 4\text{H}_2\text{O}$, $\text{Mg}(\text{NO}_3)_2 \cdot 6\text{H}_2\text{O}$ (both from VWR), $\text{Al}(\text{NO}_3)_3 \cdot 9\text{H}_2\text{O}$ and $\text{Ga}(\text{NO}_3)_3 \cdot 9\text{H}_2\text{O}$ (both from Fluka) were used to produce the LDHs. Analytical grade alcohols (1-hexanol, 1-heptanol and 1-octanol) were acquired from Sigma-Aldrich to assist the crystallization. Basic conditions were maintained by analytical grade NaOH, from VWR. High-purity 1 M HNO_3 (from Sigma-Aldrich) was used to dissolve the LDHs for chemical analysis. Concentrated NaOH (~20 M) solution was prepared and poorly soluble Na_2CO_3 was separated by filtration using CO_2 trap, then 3 M stock solutions were diluted when necessary. Other chemicals were used as received. Water was deionized by reverse osmosis.

2.2 Synthesis of layered double hydroxides

In the general method, to obtain $\text{Mg}_2\text{Al-LDH}$, $\text{Ca}_2\text{Al-LDH}$ and $\text{Ca}_2\text{Ga-LDH}$, the corresponding nitrate salts were mixed into a solution with $[\text{M}^{2+}] = 0.2 \text{ M}$ and $[\text{M}^{3+}] = 0.1 \text{ M}$, followed by addition of 3 M NaOH solution to reach $\text{pH} = 13$. The solid products were filtered after 24 h, and thoroughly washed with water, then dried at $60 \text{ }^\circ\text{C}$ overnight. The obtained LDHs will be denoted as-prepared LDHs in the followings. The syntheses were repeated with alcohol present in the reaction slurry. This is going to be called modified co-precipitation method. The solutions of the metal salts were saturated with the respective alcohol. The required volumes were calculated from literature data [32], and the saturation was indicated by tiny droplets appearing as a second phase in the aqueous solution after vigorous stirring. The approximate concentration of the 'co-solvent' was $7 \cdot 10^{-2} \text{ M}$ (1-hexanol), $1 \cdot 10^{-2} \text{ M}$ (1-heptanol) and $4 \cdot 10^{-3} \text{ M}$ (1-octanol). The separation of the LDHs was the same as for the as-prepared samples. During all processes, the nitrate solutions were purged with N_2 gas before the addition of NaOH to prevent undesired carbonation.

2.3 Instrumental analysis

Powder X-ray diffraction (XRD) patterns were collected in the range of $2\theta = 5\text{--}60^\circ$ on a Philips PW1710 diffractometer with secondary monochromator, using $\text{Cu}_{\text{K}\alpha}$ radiation and $4 \text{ }^\circ/\text{min}$ scanning step (θ is the angle of incidence of X-rays, wavelength is $\lambda = 0.1542 \text{ nm}$). X Powder software package was used for phase analysis and data evaluation. Expo2014 was used as a tool for XRD peak indexing [33] using DICLOV-06 selecting the most plausible fit, with $M20 \leq 20$. Bragg's law (SEq. 1) was applied to determine basal spacings and Scherrer's equation (SEq. 2) was used to calculate particle thickness.

Morphological studies were carried out using a Hitachi S-4700 scanning electron microscope (SEM) at various magnifications using 10 kV accelerating voltage after gold deposition on the surface of the LDH samples.

The Fourier-transform infrared (FT-IR) spectra of the samples were recorded on a JASCO FTIR-4700 spectrometer equipped with a DTGS detector in attenuated total reflectance (ZnSe ATR accessory) mode. Spectral resolution was 4 cm^{-1} , and 256 scans were collected for a spectrum. The spectra were baseline-corrected, normalized, and smoothed.

The metal ratio of the LDHs was determined after dissolution in diluted nitric acid. The obtained samples were measured by a Thermo Scientific iCAP 7400 ICP-OES DUO

spectrometer. The ICP Multi element standard solution IV acquired from CertiPUR was applied beside yttrium internal standard.

The thermal behaviour of the materials was mapped with a Setaram Labsys derivatograph. The TG-DTA (thermogravimetric-differential thermal analysis) curves were recorded under N_2 atmosphere at $3^\circ C/min$ heating rate, up to $1000^\circ C$. For the measurements, 20-30 mg sample were weighed into high-purity $\alpha-Al_2O_3$ crucibles. The resulting solids were analysed by XRD in the range of $2\theta = 5-80^\circ$.

3. Results and Discussion

For demonstration, the materials obtained with 1-hexanol as a co-solvent (or rather crystallization aiding agent) are presented, since all results obtained apply to 1-heptanol and 1-octanol as well. For characterization, primarily XRD, SEM and TG analyses were applied.

$Mg_2Al-LDH$, $Ca_2Al-LDH$ and $Ca_2Ga-LDH$ were prepared from their nitrate salts by co-precipitation to yield the corresponding materials with their XRD patterns shown in Fig. 1. While the former two are known from literature ($Mg_2Al-LDH$ and $Ca_2Al-LDH$ were associated with JCPDS cards #35-0964 and #89-6723, respectively), the XRD pattern of $Ca_2Ga-LDH$ was indexed using DICVOL-06 routine incorporated in Expo2014 program package. The indices of $Mg_2Al-LDH$ and $Ca_2Al-LDH$ were also successfully reproduced. The synthesized $Ca_2Al-LDH$ is assigned as a nitrate form; however, the $Mg_2Al-LDH$ proved to be the (mainly) hydroxide form by the paired JCPDS card. Nitrate ions are probably present in this LDH, but only in tiny amounts.

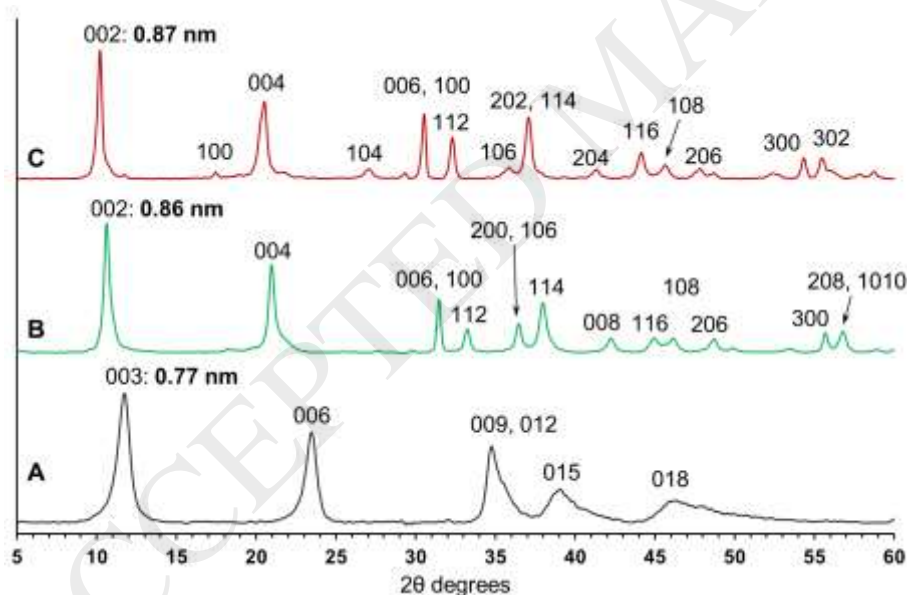


Fig. 1 XRD pattern of the as-prepared $Mg_2Al-LDH$ (A), $Ca_2Al-LDH$ (B), $Ca_2Ga-LDH$ (C) obtained by co-precipitation

In Fig. 2, the XRD patterns of the LDHs obtained by co-precipitation using 1-hexanol as a co-solvent are displayed. Relative peak intensities remain close to the original, although for the Ca-containing materials, a slight increment in the intensity ratio of $(00l)$ to other reflections (with non-zero h and k indices) may be noticed. Furthermore, these LDHs have smaller basal spacings with a difference of 0.02 nm.

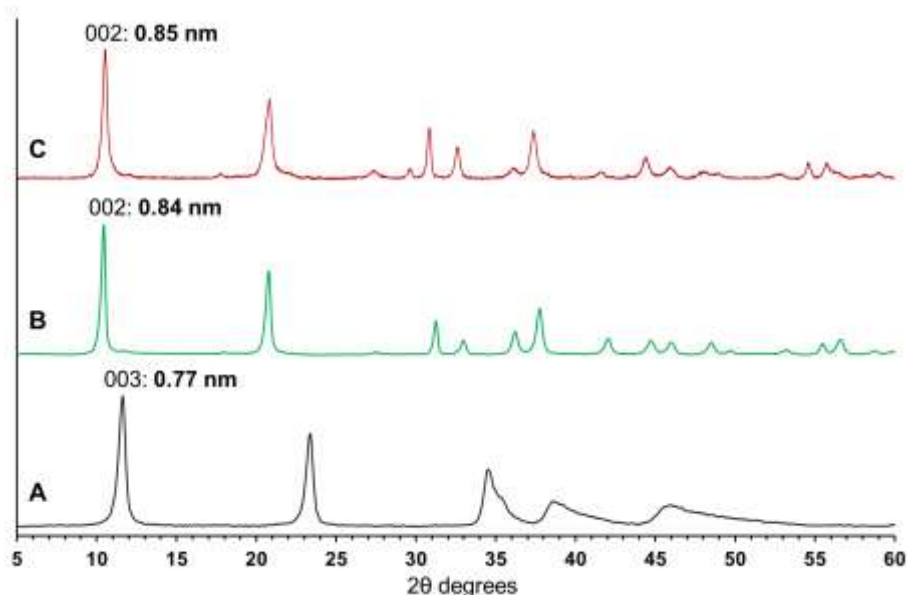


Fig. 2 XRD pattern of Mg₂Al-LDH (A), Ca₂Al-LDH (B), Ca₂Ga-LDH (C) obtained by the modified co-precipitation method (1-hexanol was also present)

The basal spacing of Mg₂Al-LDH was 0.77 nm, independently of the synthetic method used, and the profile of its XRD pattern reflects the same characteristics indicating no difference in grain thickness or morphology. After post-synthetic treatment at 60 °C, the intensity shifts for the other two LDHs were enhanced further, but no new phase appeared (Fig. 3). These characteristics foreshadow morphological changes, since the number of reflecting lattice planes correlates with the intensity of the corresponding peaks in the XRD pattern. Since (00 l) planes are those, which increase in area the most when particle diameter is risen, one can assume that the particles of the LDHs obtained from alcoholic solutions have higher particle diameter. On the contrary, Mg₂Al-LDH seems to be unaffected by the introduction of alcohols, but peak width decreased with ageing applied, displaying growth of grain thickness.

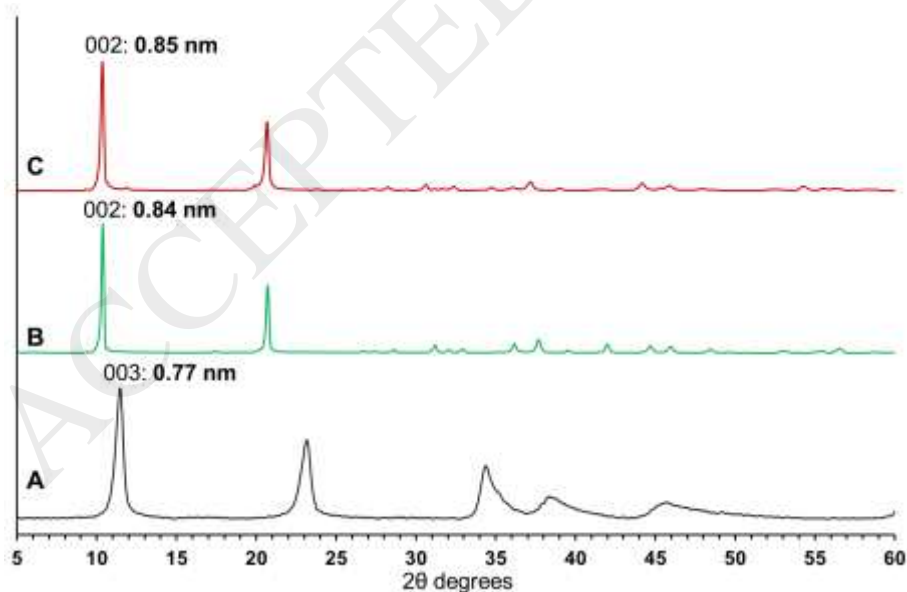


Fig. 3 XRD pattern of Mg₂Al-LDH (A), Ca₂Al-LDH (B), Ca₂Ga-LDH (C) obtained by the modified co-precipitation method (1-hexanol was also present) after weeklong ageing at 60 °C

Thermal treatment was applied on as-prepared LDHs. Comparing the X-ray patterns of such LDHs with those in Fig. 3, one may observe that Mg₂Al-LDH and Ca₂Al-LDH share similar characteristics. However, the X-ray pattern of the as-prepared and aged Ca₂Ga-LDH indicates multiphasic product (SFig. 1). We assume the formation of LDHs with different basal spacings (*e.g.* one with nitrate and the other with hydroxide as the main counter-anion), and *via* JCPDS card #26-0674, GaO(OH) by-product is also formed.

The basal spacing and the average particle thickness data of all LDH products are summarized in Table 1. As was mentioned earlier, the Mg₂Al-LDH samples had similar crystalline properties independent from the synthetic parameters, although mean particle thickness nearly tripled when ageing was introduced to the as-prepared sample. For Ca₂M-LDHs, basal spacing was reduced when alcohols were mixed with the solution of metal salts. The results fluctuate within experimental error using different alcohols. Two separate values for Ca₂Ga-LDH aged at 60 °C correspond to LDHs with different basal spacing, as mentioned earlier. Values calculated from the less intense peak are bracketed.

Table 1 Crystalline properties of the synthesized LDHs. (where ⁶⁰ does not indicate ageing at 60 °C, no change was measured after thermal treatment)

Sample	Basal spacing (nm)		Average particle thickness (nm)	
Mg ₂ Al-LDH	0.77	0.78 ⁶⁰	9	25 ⁶⁰
Mg ₂ Al-LDH with alcohol	0.77		15	
Ca ₂ Al-LDH	0.86	0.84 ⁶⁰	27	67 ⁶⁰
Ca ₂ Al-LDH with alcohol	0.84		28	48 ⁶⁰
Ca ₂ Ga-LDH	0.87	0.81 ⁶⁰ (, 0.85 ⁶⁰)	27	61 ⁶⁰ (, 31 ⁶⁰)
Ca ₂ Ga-LDH with alcohol	0.85		24	41 ⁶⁰

Generally, the interlayer distance increases when larger solvent molecules than water are situated in the interlamellar space [25,34]; nevertheless, sensitive relationship between the hydration and basal spacing of LDHs has been proven before [35]. Furthermore, starting from 1-butanol, alcohols are considered to be hydrophobic, thus after incorporation, they can reduce the H₂O content in the interlamellar space, meaning the product has lower basal spacing than the original, ‘water-rich’ LDH. Upon ageing at 60 °C, particle thickness is also increased for Ca₂M-LDHs, with 40 and 34 and 20 and 17 nm (modified co-precipitation) for the Al and the Ga analogue, respectively.

FT-IR measurements were carried out to observe the characteristic C–H vibrations around 3000 cm⁻¹, but no signals were found, probably due to the low amount of organics in the material (Fig. 4).

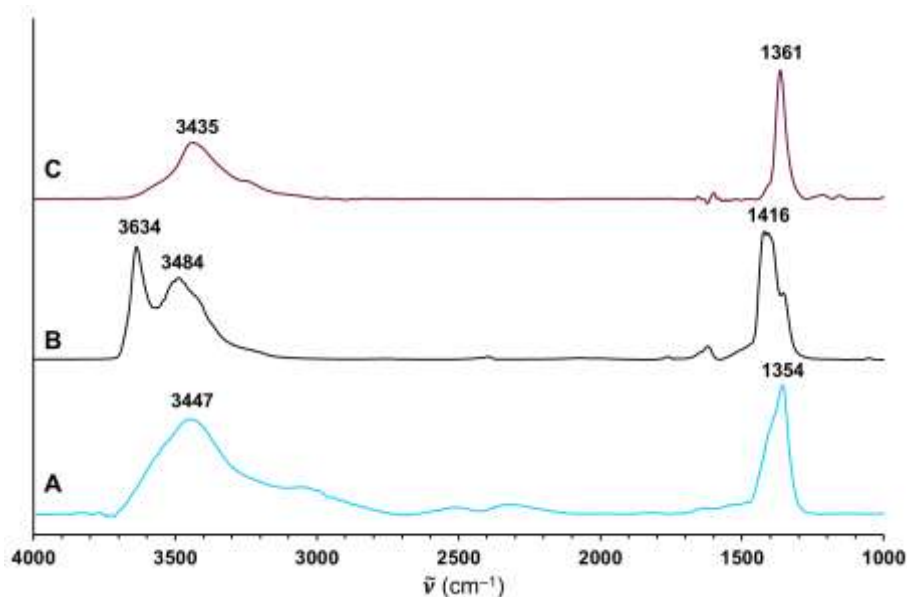


Fig. 4 FT-IR spectrum of Mg₂Al-LDH (A), Ca₂Al-LDH (B), Ca₂Ga-LDH (C) obtained by the modified co-precipitation method (1-hexanol was also present)

Bands detected in the range of 1300-1500 cm⁻¹ correspond to interlayer NO₃⁻ ions and airborne CO₂ coordinated to the surface (for Ca₂Al-LDH it is monodentate and the maximum is at 1416 cm⁻¹), while above 3200 cm⁻¹, the broad band of O-H stretching vibrations is located. For Ca₂Al-LDH, the difference between OH groups in hydrogen bonding system (maximum at 3484 cm⁻¹) and isolated OH groups (maximum at 3634 cm⁻¹) are distinguishable. For comparison, the IR spectra of the as-prepared LDHs are depicted in SFig. 2; however, relevant differences are not observable.

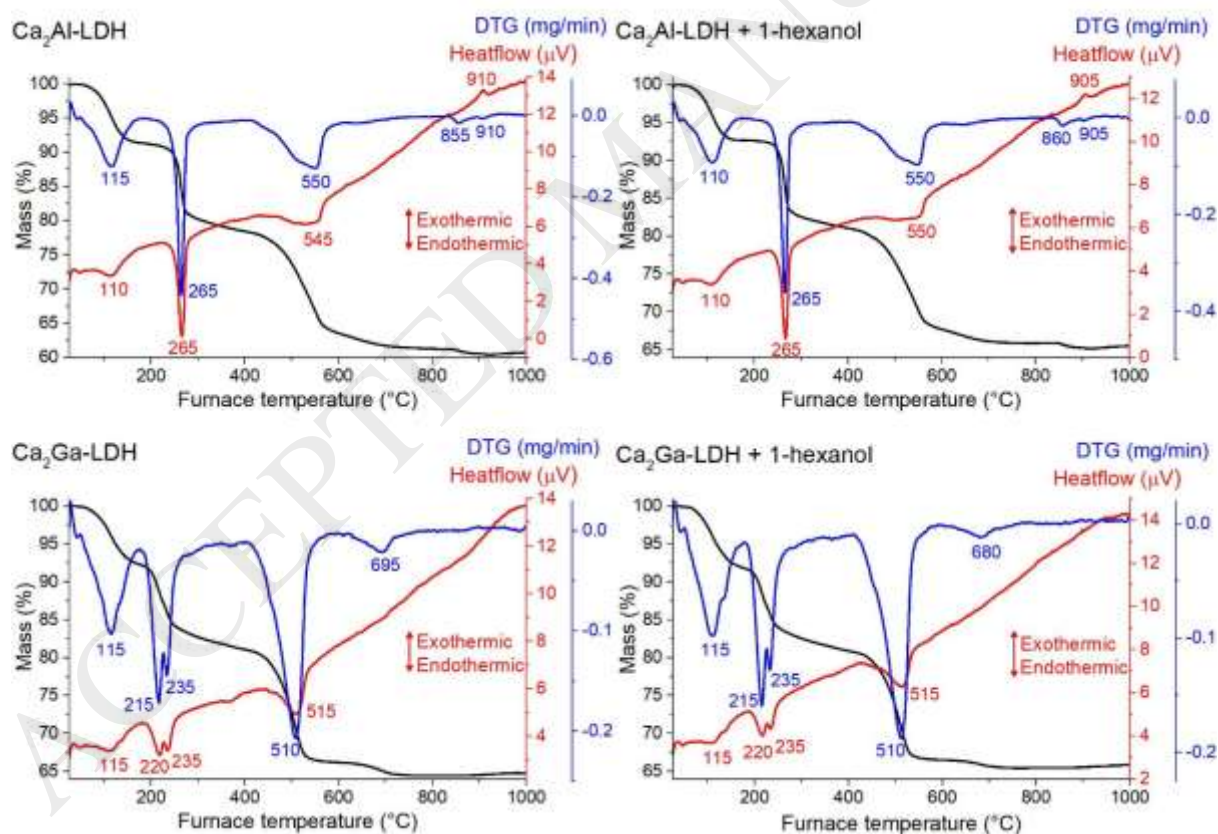
The thermal analysis of the samples prepared with and without co-solvent served with the characteristic, well-separated mass losses of the LDHs [1,36], and provide information on the alcohol-induced dehydration (Fig. 5). In the first stage, the physisorbed water molecules on the external surface of LDHs departed in the 50-150 °C temperature range. Then, the removal of interlayer water molecules took place until 300 °C. Interestingly, it occurred in two separate steps with 215 and 235 °C maxima for Ca₂Ga-LDH. Finally, the dehydroxylation of the layered metal hydroxides, and the decomposition of the interlayer NO₃⁻ ions occurred simultaneously up to 600 °C in all cases. The mass loss measured above 150 °C was significantly decreased when co-solvent was applied (Table 2). The dehydration affected the quantities of the interlayer and the structural water of the samples; the Ca₂Al-LDH was the most dehydrated one, while the alcohol had no influence on Mg₂Al-LDH (SFig. 3).

On the TGA curves, differences in mass losses are observable, but the steps appear at the same temperatures with or without alcohols. Thus, the binding energy of interlayer water molecules did not change significantly, and we conclude that the quantity of interlayer alcohol molecules is negligible compared to total mass. (Larger amounts of organic molecules should have also been indicated by IR spectroscopy.)

Table 2 Calculated mass loss values of the LDHs prepared.

Sample	Total mass loss (%)	First mass loss (%)	Second mass loss (%)	Third mass loss (%)	Fourth mass loss (%)
Mg ₂ Al-LDH	41.5	14.6	26.9	–	–
Mg ₂ Al-LDH + 1-hexanol	41.7	15.1	26.6	–	–
Ca ₂ Al-LDH	39.3	8.8	12.7	17.1	0.7
Ca ₂ Al-LDH + 1-hexanol	34.5	7.4	11.5	15.1	0.5
Ca ₂ Ga-LDH	35.3	7.7	11.1	14.8	1.7
Ca ₂ Ga-LDH + 1-hexanol	33.7	8.2	10.9	13.5	1.1

The described mass losses were exclusively connected to endothermic processes, but the DTA curves of Ca₂Al-LDH samples display an exothermic peak around 910 °C with slight nearby mass losses. The formation of spinel phase is expected at higher temperatures. Although the crystalline parameters of the aged LDHs slightly differ from those of the as-prepared ones, TG measurements show no differences.

**Fig. 5** TG-DTA curves of Ca₂Al-LDH and Ca₂Ga-LDH prepared with or without 1-hexanol

After TG analyses were concluded, the XRD pattern of the residues (denoted as LDOs) were recorded (Fig. 6). Mg₂Al-LDO consists of two materials: the classic spinel (MgAl₂O₄, ICSD #31373) and MgO (ICSD #9863). Since the metal ratio in the LDHs under investigation is M²⁺:M³⁺ = 2:1, pure spinel phase cannot be obtained from LDHs. The formation of the Ca

spinel (CaAl_2O_4 , ICSD #172781) is also observable in Fig. 6B, but another mixed oxide, mayenite ($\text{Ca}_{12}\text{Al}_{14}\text{O}_{33}$, ICSD #6287) is present in larger amount, alongside with CaO (ICSD #51409). The XRD pattern of Ca_2Ga -LDO (Fig. 6C) was covered with four products: CaO, $\text{Ca}_3\text{Ga}_4\text{O}_9$ (ICSD #100356), the corresponding spinel CaGa_2O_4 (ICSD #155955) and a polymorph of Ga_2O_3 (ICSD #236276) being the most complex and exotic heating residue out of the three LDHs. The exothermic shift on the thermal analysis curve of Ca_2Al -LDH may correspond to the formation of the spinel or the mayenite phase, since both have exothermic nature [37,38].

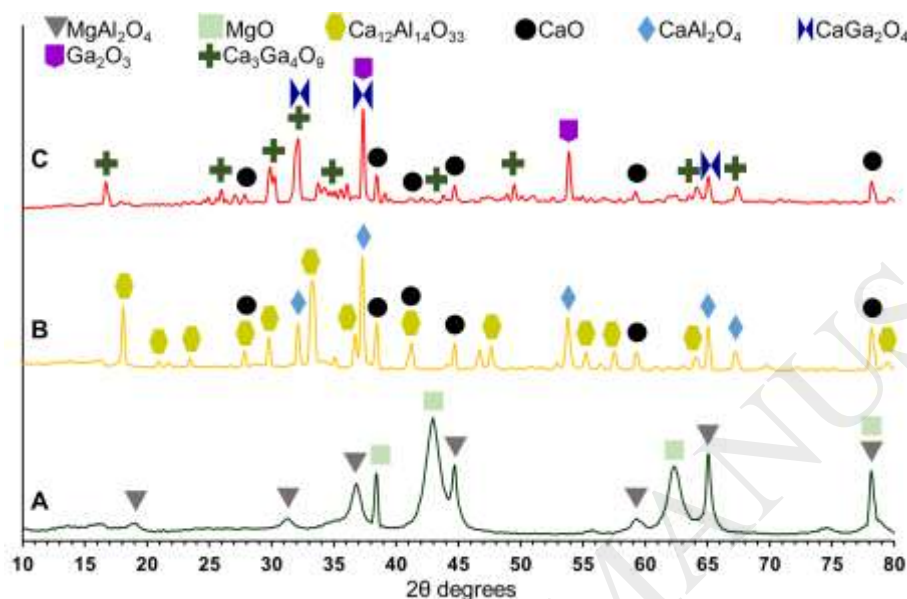


Fig. 6 XRD pattern of Mg_2Al -LDO (A), Ca_2Al -LDO (B), Ca_2Ga -LDO (C) obtained as a residue after thermogravimetric analysis

The morphological properties were investigated by SEM. For comparison, ageing was also applied for the as-prepared LDHs. It is seen that Mg_2Al -LDH contains small, grain-like particles, while the Ca-bearing LDHs have larger, plate-like crystals, typically with few hundred nm in diameter (SFig. 4). However, two substantial changes can be observed using the modified co-precipitation method (*i.e.* in the presence of alcohols): the hexagonal symmetry is more prominent, and the crystal sizes are higher (Fig. 7). These attributes become even more significant combining the modified co-precipitation method and ageing resulting in extremely rarely observed diameters of 10-15 μm for Ca_2Al -LDH and 5 μm for Ca_2Ga -LDH (Fig. 7, bottom row). In our experience, LDHs with such a well-developed morphology and large crystal size are exceptional and are complicated to produce. Morphological analysis reveals no changes for Mg_2Al -LDH. Regarding the as-prepared aged Ca_2M -LDHs, their typical size range is between 5-10 μm in diameter; however, the hexagonal symmetry is broken by big cracks and fragmentations, *i.e.* the crystals have rough surface and edges (SFig 4, bottom row), compared to the smooth and symmetrical crystals obtained by the modified co-precipitation method.

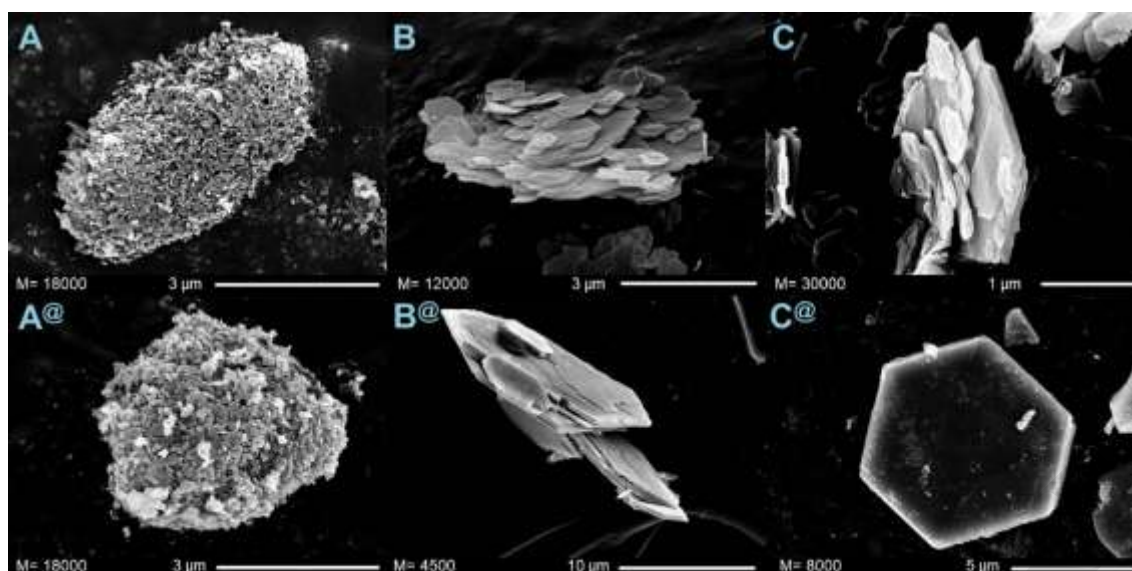


Fig. 7 SEM micrographs of $\text{Mg}_2\text{Al-LDH}$ (A), $\text{Ca}_2\text{Al-LDH}$ (B), $\text{Ca}_2\text{Ga-LDH}$ (C) obtained by the modified co-precipitation (in the presence of 1-hexanol) without (no symbol) and after weeklong ageing at $60\text{ }^\circ\text{C}$ (@)

LDHs containing Ca are known for their coordination number of 7 around the Ca^{2+} centres, while Mg^{2+} and Al^{3+} ions have octahedral geometry. The extra coordination site is occupied by an interlamellar H_2O molecule. With the introduction of alcohols, the replacement of H_2O molecules with the alcohol molecules around the Ca^{2+} ions is plausible, *i.e.* we attribute the lack of morphological change for $\text{Mg}_2\text{Al-LDH}$ to the lack of the extra coordination site of the component ions.

The metal composition of the LDHs was determined (Table 3) and we conclude that the presence of the co-solvent did not modify the metal content of the lamellae, thus the textural and morphological changes of the Ca-based LDHs are results of the coordination of the alcohols, not the formation of a different LDH phase.

Table 3 Metal ratios of the LDHs prepared.

Sample	$\text{M}^{2+}:\text{M}^{3+}$ metal ratio (atom%)	
	As-prepared	Modified co-precipitation
$\text{Mg}_2\text{Al-LDH}$	2.02	2.03
$\text{Ca}_2\text{Al-LDH}$	2.06	2.04
$\text{Ca}_2\text{Ga-LDH}$	2.05	2.01

4. Conclusions

The synthesis of pure LDHs ($\text{Mg}_2\text{Al-LDH}$, $\text{Ca}_2\text{Al-LDH}$ and $\text{Ca}_2\text{Ga-LDH}$) was performed by co-precipitation with partially miscible alcohols (1-hexanol, 1-heptanol or 1-octanol) present in the starting nitrate solution as co-solvent. The alcohols, applied in saturated concentration, acted as powerful crystallization-aiding agents. The effect of post-synthetic ageing was also investigated. $\text{Mg}_2\text{Al-LDH}$ was mostly unaffected by the alcohols, the grain-like morphology remained; however, the grain thickness increased. Regarding the Ca-bearing materials, the diameter of the hexagonal platelets rose from *ca.* 200 nm to 1-3 μm with no thermal treatment

and to an exceptional 5-10 μm after ageing at 60 $^{\circ}\text{C}$ for a week, and the improvement in their hexagonal symmetry was also observable. When ageing was applied without alcohols, the platelets were covered with cracks and fragmentation occurred. This phenomenon was inhibited by the co-solvents. Our method is a convenient and facile route to produce LDHs with large and symmetrical crystals. The differences in the distinct morphologic changes is attributed to structural motifs, since Ca^{2+} ions are capable of coordinating seven ligands, one of them being a solvent molecule, most probably alcohol located between the layers. While it has been published that organics can affect the properties of the LDHs if present at higher concentrations, it is the first occasion to observe such a change with low co-solvent concentration. It seems that applied alcohols, after coordinating to the structure-building Ca^{2+} ions lead to a preferred crystal growth in lateral dimensions resulting in crystals with high aspect ratio and smooth surface. The Ca-based LDHs, obtained by the modified synthesis have lower basal spacing than the as-prepared materials, since alcohol is present between the layers after synthesis excluding a small portion of water, leading to a partially dehydrated material, confirmed *via* TG measurements. Novel results also include the description of thermal behaviour of Ca_2Ga -LDH. The obtained mixed oxides were characterized by XRD and the diffraction peaks were assigned to various oxides.

Acknowledgement

This study was supported by the European Union and the Government of Hungary through grant GINOP-2.3.2-15-2016-00013 (MS, PS, IP), by the Lendület program of the Hungarian Academy of Sciences (96130), by the Ministry of Human Capacities, Hungary through grant 20391-3/2018/FEKUSTRAT (SM, IS) and by the János Bolyai Research Scholarship of the Hungarian Academy of Sciences (DS). The financial help is highly appreciated. The authors are grateful for Marianna Kocsis for her assist in the preparation of NaOH solutions.

Conflict of interest

The authors declare no conflict of interest.

References

- [1] F. Cavani, F. Trifirò, A. Vaccari, Hydrotalcite-type anionic clays: Preparation, properties and applications., *Catal. Today* 11 (1991) 173–301. [https://doi.org/10.1016/0920-5861\(91\)80068-K](https://doi.org/10.1016/0920-5861(91)80068-K)
- [2] S.J. Mills, A.G. Christy, J.-M.R. Génin, T. Kameda, F. Colombo, Nomenclature of the hydrotalcite supergroup: natural layered double hydroxides, *Mineral. Mag.* 76(5) (2012) 1289–1336. <https://doi.org/10.1180/minmag.2012.076.5.10>
- [3] V. Rives, M.A. Ulibarri, Layered double hydroxides (LDH) intercalated with metal coordination compounds and oxometalates, *Coordin. Chem. Rev.* 181 (1999) 61–120. [https://doi.org/10.1016/S0010-8545\(98\)00216-1](https://doi.org/10.1016/S0010-8545(98)00216-1)
- [4] S.P. Newman, W. Jones, Synthesis, characterization and applications of layered double hydroxides containing organic guests, *New J. Chem.* 22 (1998) 105–115. <https://doi.org/10.1039/A708319J>
- [5] Z. Gu, S. Yan, S. Cheong, Z. Cao, H. Zuo, A.C. Thomas, B.E. Rolfe, Z.P. Xu, Layered double hydroxide nanoparticles: Impact on vascular cells, blood cells and the complement system, *J. Colloid Interf. Sci.* 512 (2018) 404–410. <https://doi.org/10.1016/j.jcis.2017.10.069>.
- [6] F.R. Costa, M. Saphiannikova, U. Wagenknecht, G. Heinrich, Layered Double Hydroxide Based Polymer Nanocomposites, *Adv. Polym. Sci.* 210 (2008) 101–168. https://doi.org/10.1007/12_2007_123
- [7] Y. Cao, G. Li, X. Li, Graphene/layered double hydroxide nanocomposite: Properties, synthesis, and applications, *Chem. Eng. J.* 292 (2016) 207–223. <https://doi.org/10.1016/j.cej.2016.01.114>
- [8] M. Zubair, M. Daud, G. McKay, F. Shehzad, M.A. Al-Harthi, Recent progress in layered double hydroxides (LDH)-containing hybrids as adsorbents for water remediation, *Appl. Clay Sci.* 143 (2017) 279–292. <https://doi.org/10.1016/j.clay.2017.04.002>
- [9] D. Tichit, C. Gérardin, R. Durand, B. Coq, Layered double hydroxides: precursors for multifunctional catalysts, *Top. Catal.* 39 (2006) 89–96. <https://doi.org/10.1007/s11244-006-0041-6>
- [10] K.A. Tarasov, D. O'Hare, Solid-State Chelation of Metal Ions by Ethylenediaminetetraacetate Intercalated in a Layered Double Hydroxide, *Inorg. Chem.* 42 (2003) 1919–1927. <https://doi.org/10.1021/ic0203926>
- [11] S.I. Garcés-Polo, J. Villaroel-Rocha, K. Sapag, S.A. Korili, A. Gil, Adsorption of CO₂ on mixed oxides derived from hydrotalcites at several temperatures and high pressures, *Chem. Eng. J.* 332 (2018) 24–32. <https://doi.org/10.1016/j.cej.2017.09.056>
- [12] Z.P. Xu, J. Zhang, M.O. Adebajo, H. Zhang, C. Zhou, Catalytic applications of layered double hydroxides and derivatives, *Appl. Clay. Sci.* 53 (2011) 139–150. <https://doi.org/10.1016/j.clay.2011.02.007>
- [13] U. Constantino, V. Ambrogi, M. Nocchetti, L. Perioli, Hydrotalcite-like compounds: Versatile layered hosts of molecular anions with biological activity, *Micropor. Mesopor. Mat.* 107 (2008) 149–160. <https://doi.org/10.1016/j.micromeso.2007.02.005>
- [14] L. Li, Q. Chen, Q. Zhang, J. Shi, Y. Li, W. Zhao, J. Shi, Layered double hydroxide confined Au colloids: High performance catalysts for low temperature CO oxidation, *Catal. Commun.* 26 (2012) 15–18. <https://doi.org/10.1016/j.catcom.2012.04.025>

- [15] S. Han, X. Chang, D. Wu, H. Chen, D. Chen, P. Liu, T. Huang, X. Jiang, Q. Huang, H. Lin, Hierarchically porous cobalt aluminum layered double hydroxide flowers with enhanced capacitance performances, *J. Mater. Sci.* 52 (2017) 6081–6092. <https://doi.org/10.1007/s10853-017-0847-6>
- [16] T. Posati, F. Bellezza, A. Cipiciani, F. Constantino, M. Nocchetti, L. Tarpani, L. Latterini, Synthesis and Characterization of Luminescent Nanoclays, *Crys. Growth Des.* 10 (2010) 2847–2850. <https://doi.org/10.1021/cg100100a>
- [17] M. Pavlovic, P. Rouster, I. Szilágyi, Synthesis and formulation of functional bionanomaterials with superoxide dismutase activity, *Nanoscale* 9 (2017) 369–379. <https://doi.org/10.1039/C6NR07672F>
- [18] O. Rahmanian, M.H. Maleki, M. Dinari, Ultrasonically assisted solvothermal synthesis of novel Ni/Al layered double hydroxide for capturing of Cd(II) from contaminated water, *J. Phys. Chem. Solids* 110 (2017) 195–201. <https://doi.org/10.1016/j.jpcs.2017.06.018>
- [19] T. Hibino, H. Ohya, Synthesis of crystalline layered double hydroxides: Precipitation by using urea hydrolysis and subsequent hydrothermal reactions in aqueous solutions, *Appl. Clay Sci.* 45 (2009) 123–132. <https://doi.org/10.1016/j.clay.2009.04.013>
- [20] M.R. Berber, I.H. Hafez, K. Minagawa, M. Katoh, M. Tanaka, T. Mori, Control of nanoparticle size, crystal structure and growth of layered double hydroxide by hydrothermal treatment, *Int. J. Mod. Phys. Conf. Ser.* 6 (2012) 133–137. <https://doi.org/10.1142/S2010194512003066>
- [21] J.-M. Oh, S.-H. Hwang, J.-H. Choy, The effect of synthetic conditions on tailoring the size of hydrocalcite particles, *Solid State Ionics* 151 (2002) 285–291. [https://doi.org/10.1016/S0167-2738\(02\)00725-7](https://doi.org/10.1016/S0167-2738(02)00725-7)
- [22] I. Clark, P.W. Dunne, R.L. Gomes, E. Lester, Continuous hydrothermal synthesis of Ca₂Al-NO₃ layered double hydroxides: The impact of reactor temperature, pressure and NaOH concentration on crystal characteristics, *J. Colloid. Interf. Sci.* 504 (2017) 492–499. <https://doi.org/10.1016/j.jcis.2017.05.105>
- [23] M. François, G. Renaudin, O. Evrard, A Cementitious Compound with Composition 3CaO·Al₂O₃·CaCO₃·11H₂O, *Acra Cryst.* C54 (1998) 1214–1217. <https://doi.org/10.1107/S0108270198004223>
- [24] G. Renaudin, M. François, The lamellar double-hydroxide (LDH) compound with composition 3CaO·Al₂O₃·Ca(NO₃)₂·10H₂O, *Acra Cryst* C55 (1999) 835–838. <https://doi.org/10.1107/S0108270199003066>
- [25] J. Wang, Y. Wei, J. Yu, Influences of polyhydric alcohol co-solvents on the hydration and thermal stability of MgAl-LDH obtained via hydrothermal synthesis, *Appl. Clay Sci.* 72 (2013) 37–43. <https://doi.org/10.1016/j.clay.2013.01.006>
- [26] X. Meng, M. Feng, H. Zhang, Z. Ma, C. Zhang, Solvothermal synthesis of cobalt/nickel layered double hydroxides for energy storage devices, *J. Alloy. Compd.* 695 (2017) 3522–3529. <https://doi.org/10.1016/j.jallcom.2016.11.419>
- [27] Y. Zhang, L. Wang, L. Zou, D. Xue, Crystallization behaviours of hexagonal nanoplatelet MgAl-CO₃ layered double hydroxide, *J. Cryst. Growth* 312 (2010) 3367–3372. <https://doi.org/10.1016/j.jcrysgro.2009.10.068>

- [28] J. Karthikeyan, H. Fjellvåg, Ø.B. Vistad, K.D. Knudsen, A. Olafsen Sjøstad, Quantification and key factors in delamination of $(\text{Mg}_{1-y}\text{Ni}_y)_{1-x}\text{Al}_x(\text{OH})_2(\text{NO}_3)_x \cdot m\text{H}_2\text{O}$, *Appl. Clay Sci.* 124-125 (2016) 102–110. <https://doi.org/10.1016/j.clay.2016.02.001>
- [29] M. Adachi-Pagano, C. Forano, J.-P. Besse, Delamination of layered double hydroxides by use of surfactants, *Chem. Commun.* 0 (2000) 91–92. <https://doi.org/10.1039/A908251D>
- [30] S. Muráth, Z. Somosi, I.Y. Tóth, E. Tombácz, P. Sipos, I. Pálkó, Delaminating and restacking MgAl-layered double hydroxide monitored and characterized by a range of instrumental methods, *J. Mol. Struct.* 1140 (2017) 77–82. <https://doi.org/10.1016/j.molstruc.2016.10.056>
- [31] I. Rousselot, C. Taviot-Guého, F. Leroux, P. Léone, P. Palvadeau, J.-P. Besse, Insights on the Structural Chemistry of Hydrocalumite and Hydrotalcite-like Materials: Investigation of the Series $\text{Ca}_2\text{M}^{3+}(\text{OH})_6\text{Cl} \cdot 2\text{H}_2\text{O}$ (M^{3+} : Al^{3+} , Ga^{3+} , Fe^{3+} , and Sc^{3+}) by X-Ray Powder Diffraction, *J. Solid State Chem.* 167 (2002) 137–144. <https://doi.org/10.1006/jssc.2002.9635>
- [32] S.H. Yalkowsky, Y. He, P. Jain, *Handbook of Aqueous Solubility Data*, second ed., CRC Press, Boca Raton, 2010.
- [33] A. Altomare, C. Cuocci, C. Giacobozzo, A. Moliterni, R. Rizzi, N. Corriero, A. Falcicchio, EXPO2013: a kit of tools for phasing crystal structures from powder data. *J. Appl. Crystallogr.* 46 (2013) 1231–1235. <https://doi.org/10.1107/S0021889813013113>
- [34] J.S. Valente, M.S. Cantú, J.G.H. Cortez, R. Montiel, X. Bokhimi, E. López-Salinas, Preparation and Characterization of Sol–Gel MgAl Hydrotalcites with Nanocapsular Morphology, *J. Phys. Chem. C* 111 (2007) 642–651. <https://doi.org/10.1021/jp065283h>
- [35] N. Iyi, K. Fujii, K. Okamoto, T. Sasaki, Factors influencing the hydration of layered double hydroxides (LDHs) and the appearance of an intermediate second staging phase, *Appl. Clay Sci.* 35 (2007) 218–227. <https://doi.org/10.1016/j.clay.2006.08.011>
- [36] C. Forano, T. Hibino, F. Leroux, C. Taviot-Guého, Layered double hydroxides, *Developments in Clay Science* 1 (2006) 1021–1095. [https://doi.org/10.1016/S1572-4352\(05\)01039-1](https://doi.org/10.1016/S1572-4352(05)01039-1)
- [37] J.S. Valente, G. Rodriguez-Gattorno, M. Valle-Orta, E. Torres-Garcia, Thermal decomposition kinetics of MgAl layered double hydroxides, *Mater. Chem. Phys.* 133 (2012) 621–629. <https://doi.org/10.1016/j.matchemphys.2012.01.026>
- [38] J. Huang, L. Valenzano, G. Sant, Framework and Channel Modifications in Mayenite ($12\text{CaO} \cdot 7\text{Al}_2\text{O}_3$) Nanocages By Cationic Doping, *Chem. Mater.* 27 (2015) 4731–4741. <https://doi.org/10.1021/acs.chemmater.5b01360>